

Supporting Information

Rational Molecular Design of Highly Efficient Yellow-red Thermally Activated Delayed Fluorescent Emitters: A combined Effect of Auxiliary Fluorine and Rigidified Acceptor Unit

*Shantaram Kothavale, Won Jae Chung, Jun Yeob Lee**

*School of Chemical Engineering, Sungkyunkwan University
2066, Seobu-ro, Jangan-gu, Suwon, Gyeonggi, 440-746, Korea*

E-mail: leej17@skku.edu

Table of contents	Page No
Figure. S1. DFT optimized structures of FDQCNAC and FBPCNAC with respective dihedral angles between donor and acceptor unit.	S-7
Figure S2. Thermogravimmetric analysis (TGA) curves of two emitters.	S-8
Figure S3. DSC thermograms of FDQCNAC and FBPCNAC TADF emitters.	S-9
Figure S4. Cyclic voltammograms of TADF emitters FDQCNAC and FBPCNAC	S-10
Figure S5. EQE–luminance curves of FDQCNAC doped OLED (1-5 %)	S-11
Figure S6. EL spectra of FDQCNAC at 1-5 % doping concentration	S-12
Figure S7. EQE–luminance curves of FBPCNAC doped OLED (1-5 %)	S-13
Figure S8. EL spectra of FBPCNAC at 1-5 % doping concentration	S-14
Figure S9. ¹ H NMR spectrum of Intermediate 1	S-15
Figure S10. ¹³ C NMR spectrum of Intermediate 1	S-16
Figure S11. ¹ H NMR spectrum of Intermediate 2	S-17
Figure S12. ¹³ C NMR spectrum of Intermediate 2	S-18
Figure S13. ¹ H NMR spectrum of Intermediate 4	S-19
Figure S14. ¹³ C NMR spectrum of Intermediate 4	S-20
Figure S15. ¹ H NMR spectrum of FDQCNAC	S-21
Figure S16. ¹³ C NMR spectrum of FDQCNAC	S-22
Figure S17. ¹ H NMR spectrum of FBPCNAC	S-23
Figure S18. ¹³ C NMR spectrum of FBPCNAC	S-24

Figure S19. HPLC report of FDQCNAC after sublimation.	S-25
Figure S20. HPLC report of FDQCNAC after sublimation.	S-25
Figure S21. HRMS report of FDQCNAC.	S-26
Figure S22. HRMS report of FBPCNAC.	S-27
Equations for the calculation of rate constants	S-28

Experimental

General Information

4,5-Difluorobenzene-1,2-diamine and 9,9-dimethyl-9,10-dihydroacridine were purchased from P&H tech. 4,4'-Dibromobenzil was acquired from Sigma Aldrich. Copper cyanide (CuCN) was purchased from Alfa Aesar. Sodium hydride (NaH) was purchased from Tokyo Chemical Industry (TCI) Ltd. *N,N* dimethyl formamide (DMF) and acetic acid were obtained from Duksan Sci. Co. All these chemicals were used without further purification. Column chromatography (Silica Gel 60, 230–400 mesh, Merck) and sublimation (10^{-3} Torr at 300 °C) purification processes were used to obtain pure products before applying for OLED devices.

The ^1H and ^{13}C nuclear magnetic resonance (NMR) spectra were recorded in deuterated chloroform (CDCl_3) solution on an Avans 500 MHz spectrometer. Chemical shifts of the ^1H and ^{13}C NMR signals were quoted relative to tetramethylsilane ($\delta = 0.00$). All coupling constants are reported in Hertz. The ultraviolet–visible (UV–vis) spectra were obtained using a UV–vis spectrophotometer (JASCO, Easton, MD; V-730), and the photoluminescence (PL) spectra were recorded on a fluorescence spectrophotometer (PerkinElmer, Waltham, MA; LS55). CV measurement was carried out in dichloromethane solution with scan rate at 100 mV/s. The glassy carbon, platinum wire and Ag/AgCl were used as working, counter and reference electrodes respectively. Internal standard was ferrocenium/ferrocene couple and supporting electrolyte was 0.1 M tetrabutylammonium perchlorate (TBAClO_4). The mass spectra were recorded using aAdvion, Expression LCMS spectrometer in APCI mode. Absolute photoluminescence quantum yields (PLQYs) of 1 wt % doped polystyrene film solid film were measured with a Hamamatsu

Quantaaurus-QY C11347-11 spectrometer under a nitrogen atmosphere condition. The transient photoluminescence decay characteristics of solid film samples were recorded using a Quantaaurus-Tau fluorescence lifetime measurement system (C11367-31, Hamamatsu Photonics).

Device Fabrication and Measurements

The device structure was indium tin oxide (ITO, 50 nm)/poly(3,4-ethylenedioxythiophene):poly(styrenesulfonate) (PEDOT:PSS, 60 nm)/4,4'-cyclohexylidenebis[N,N-bis(4-methylphenyl)aniline] (TAPC, 20 nm)/1,3-bis(N-carbazolyl)benzene (mCP, 10 nm)/ 2-phenyl-4,6-bis(12-phenylindolo[2,3-a]carbazole-11-yl) - 1,3,5-triazine(PBICT):dopant (25 nm; 1, 3 and 5 wt%)/diphenylphosphine oxide-4-(triphenylsilyl)phenyl (TSPO1, 5 nm)/2,2',2''-(1,3,5-benzinetriyl)-tris(1-phenyl-1-H-benzimidazole) (TPBi) (40 nm)/LiF(1.5 nm)/Al(200 nm). The dopants were FDQCNAC and FBPCNAC. All layers of the device structure were deposited by vacuum thermal evaporation under a high pressure of 3.0×10^{-7} Torr. The material was thermally evaporated and then encapsulated with a glass lid in a nitrogen-filled glove box to protect the device from moisture and oxygen. Electrical characterization of the devices was performed using a Keithley 2400 source meter and optical characterization was carried out using a CS 2000 spectroradiometer.

Synthesis of 2,3-bis(4-bromophenyl)-6,7-difluoroquinoxaline (1)

4,5-Difluorobenzene-1,2-diamine (2.5 g, 17.34 mmol) and 1,2-bis(4-bromophenyl)ethane-1,2-dione (6.38 g, 17.34 mmol) were dissolved in glacial acetic acid (80 mL) and the reaction mixture was refluxed for 12 h. Solid precipitated out after cooling to room temperature was filtered and dried well as a pure product (5.3 g, 64.24 %). MS (FAB) m/z 474 [(M + H)⁺].

Synthesis of 10-(2,3-bis(4-bromophenyl)-7-fluoroquinoxalin-6-yl)-9,9-dimethyl-9,10-dihydroacridine (2)

9,9-Dimethyl-9,10-dihydroacridine (0.79 g, 3.78 mmol) was dissolved in N,N-dimethylformamide (30 mL) and cooled to 0°C. Sodium hydride (0.22 g, 4.72 mmol, 55 wt %) was added to the solution and the mixture was stirred for 1 h. Then, 2,3-bis(4-bromophenyl)-6,7-difluoroquinoxaline (1) (5.3 g, 11.34 mmol) was added to the mixture and the reaction mixture was stirred for 12 h. The mixture was poured into water and extracted with dichloromethane. The organic phase was washed with water and dried with anhydrous sodium sulfate. The solvent was removed under reduced pressure to give the crude product, which was purified by column chromatography (silica gel, hexane/ethyl acetate) to give the pure product (2) (1.2 g, 10 %).

was added slowly in the reaction mixture and stirred for 1 hr at room temperature. Reaction mixture was again cooled to 0 °C. 2,3-Bis(4-bromophenyl)-6,7-difluoroquinoxaline (1.5 g, 3.15 mmol) was added slowly in the reaction mixture and was stirred at 70 °C for 8 h. After cooling to room temperature, water was added in the reaction mixture. The solid precipitated out was filtered and dried well. The crude product obtained was further purified by column chromatography (20 % DCM in hexane) to afford desired product as a yellow solid (1.3 g, 62.20 %). MS (FAB) m/z 664 $[(M + H)^+]$. 1H NMR (300 MHz, $CDCl_3$): δ 8.32-8.33 (d, J = 8 Hz, 1H), 8.06-8.08 (d, J = 9 Hz, 1H), 7.51-7.56 (m, 6H), 7.41-7.46 (m, 4H), 6.99-7.01 (m, 4H), 6.37-6.39 (m, 2H), 1.74 (s, 6H). ^{13}C NMR (125 MHz, $CDCl_3$): δ 162.5, 160.7, 153.5, 152.1, 142.1, 142.0, 140.0, 139.4, 137.3, 134.5, 133.0, 132.9, 132.1, 132.0, 131.6, 131.5, 130.9, 126.8, 125.6, 124.5, 124.3, 121.8, 115.6, 115.4, 113.6, 36.3, 30.9.

Synthesis of 3,6-dibromo-11,12-difluorodibenzo[a,c]phenazine (3)

Same procedure as described for the synthesis of intermediate 1 was followed to obtain 7.5 g (91.24 %) pure product. MS (FAB) m/z 472 $[(M + H)^+]$.

Synthesis of 3,6-dibromo-11-(9,9-dimethylacridin-10(9H)-yl)-12-fluorodibenzo[a,c]phenazine (4)

The same procedure as described for the synthesis of intermediate 2 was followed to obtain 1.2 g (63.16 %) pure product. MS (FAB) m/z 662 $[(M + H)^+]$. 1H NMR (300 MHz, $CDCl_3$): δ 9.17-9.15 (d, J = 8.5 Hz, 1H), 9.05-9.07 (d, J = 8.5 Hz, 1H), 8.45-8.47 (m, 3H), 8.14-8.16 (d, J = 9 Hz, 1H), 7.83-7.85 (d, J = 8.5 Hz, 1H), 7.78-7.80 (d, J = 8.5 Hz, 1H), 7.53-7.55 (m, 2H), 7.01-7.03 (m, 4H), 6.45-6.46 (m, 2H), 1.77 (s, 6H). ^{13}C NMR (125 MHz, $CDCl_3$): δ 143.1, 142.9, 142.6, 141.5, 140.4, 140.1, 134.7, 132.7, 132.4, 132.1, 130.9, 129.1, 129.0, 128.4, 128.1, 126.8, 126.4, 126.2, 126.1, 126.0, 125.6, 121.8, 115.3, 115.1, 113.7, 36.4, 31.1.

Synthesis of 4,4'-(6-(9,9-dimethylacridin-10(9H)-yl)-7-fluoroquinoxaline-2,3-diyl)dibenzonitrile (**FDQCNAc**)

10-(2,3-Bis(4-bromophenyl)-7-fluoroquinoxalin-6-yl)-9,9-dimethyl-9,10-dihydroacridine (0.9 g, 1.35 mmol) was dissolved in N,N dimethylformamide (50 mL). Copper cyanide (0.6 g, 6.76 mmol) was added and the reaction mixture was refluxed for 12 h. After cooling to room temperature, water was added in the reaction mixture. Solid precipitated out was filtered and dried well. The crude product was further purified with column chromatography (50 % DCM in hexane) to obtain pure product (0.38 g, 50.66 %). ¹H NMR (500 MHz, CDCl₃): δ 8.37-8.39 (d, *J* = 7.5 Hz, 1H), 8.10-8.12 (d, *J* = 9.5 Hz, 1H), 7.64-7.73 (m, 8H), 7.52-7.54 (m, 2H), 6.99-7.03 (m, 4H), 6.36-6.38 (m, 2H), 1.74 (s, 6H). ¹³C NMR (125 MHz, CDCl₃): δ 163.1, 161.1, 152.4, 151.0, 142.4, 139.9, 139.6, 134.8, 134.1, 133.9, 132.6, 131.1, 130.8, 126.8, 125.7, 122.0, 118.3, 115.8, 115.6, 113.8, 113.6, 36.4, 31.0. MS (FAB) *m/z* 558 [(M + H)⁺]. HRMS: (M+H)⁺, C₃₇H₂₄FN₅, calcd, 558.2094; found 558.2094.

Synthesis of 11-(9,9-dimethylacridin-10(9H)-yl)-12-fluorodibenzo[a,c]phenazine-3,6-dicarbonitrile (**FBPCNAc**)

Same procedure as described above for the synthesis of FDQCNAc was followed to obtain 0.32 g (47.76 %) pure product. ¹H NMR (500 MHz, CDCl₃): δ 9.56-9.58 (d, *J* = 8.5 Hz, 1H), 9.46-9.48 (d, *J* = 8.5 Hz, 1H), 8.85-8.87 (d, *J* = 9.5 Hz, 2H), 8.45 (s, 1H), 8.06-8.08 (d, *J* = 8.5 Hz, 1H), 7.99-8.01 (d, *J* = 8.5 Hz, 1H), 7.83 (s, 1H), 7.51-7.53 (m, 2H), 6.96-7.00 (m, 4H), 6.41-6.43 (m, 2H), 1.76 (s, 6H). ¹³C NMR (125 MHz, CDCl₃): δ 159.7, 144.7, 141.5, 140.1, 139.7, 139.3, 136.9, 134.3, 133.8, 131.3, 131.1, 130.8, 130.1, 127.8, 127.7, 127.5, 127.1, 126.5, 125.4, 121.3, 118.8, 118.7, 114.3, 113.8, 113.6, 108.9, 36.3, 14.4. MS (FAB) *m/z* 556 [(M + H)⁺]. HRMS: (M+H)⁺, C₃₇H₂₂FN₅, calcd, 556.1937; found 556.1937.

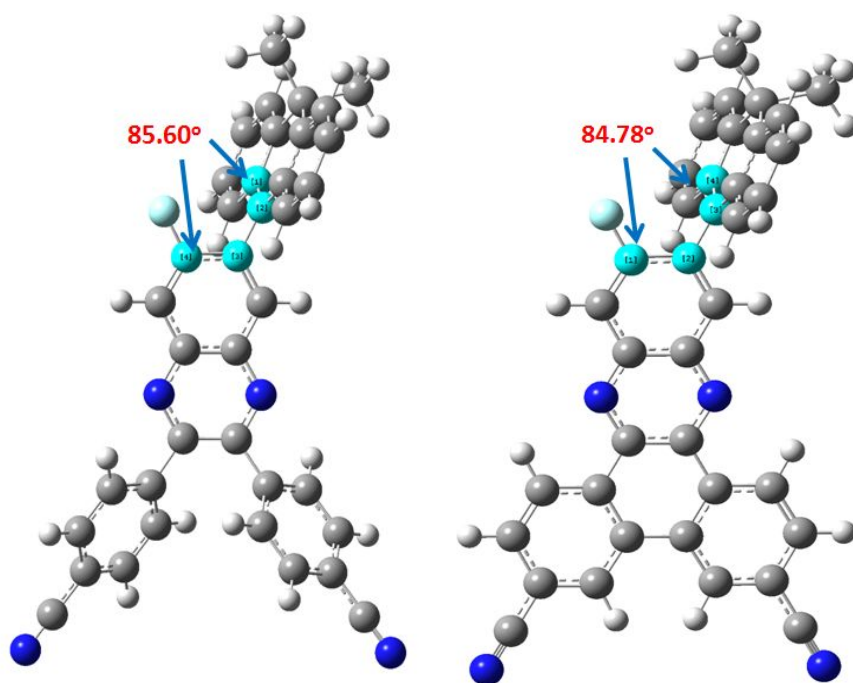


Figure. S1. DFT optimized structures of FDQCNac and FBPCNac with respective dihedral angles between donor and acceptor unit.

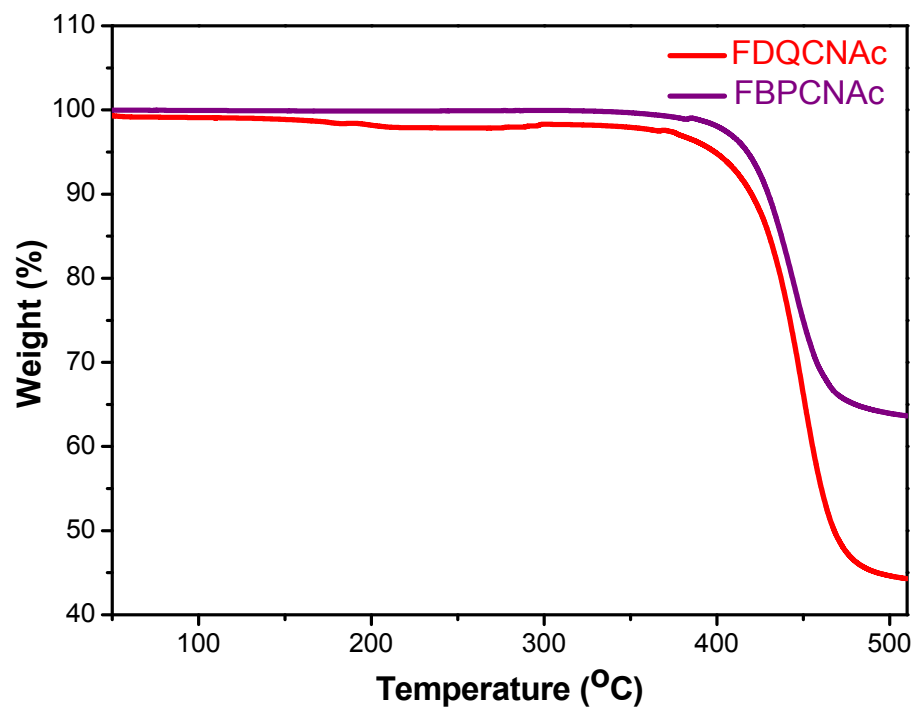


Figure S2. Thermogravimmetric analysis (TGA) curves of two emitters under nitrogen.

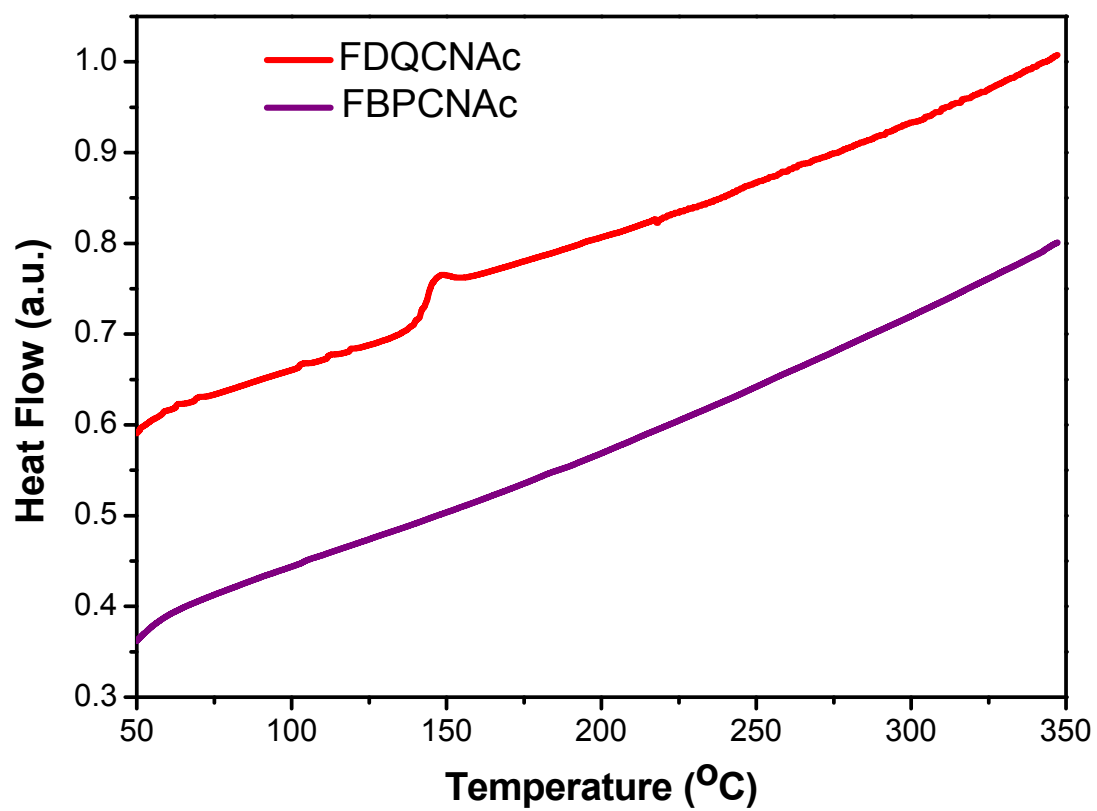


Figure S3. DSC thermograms of FDQCNAc and FBPCNAc TADF emitters.

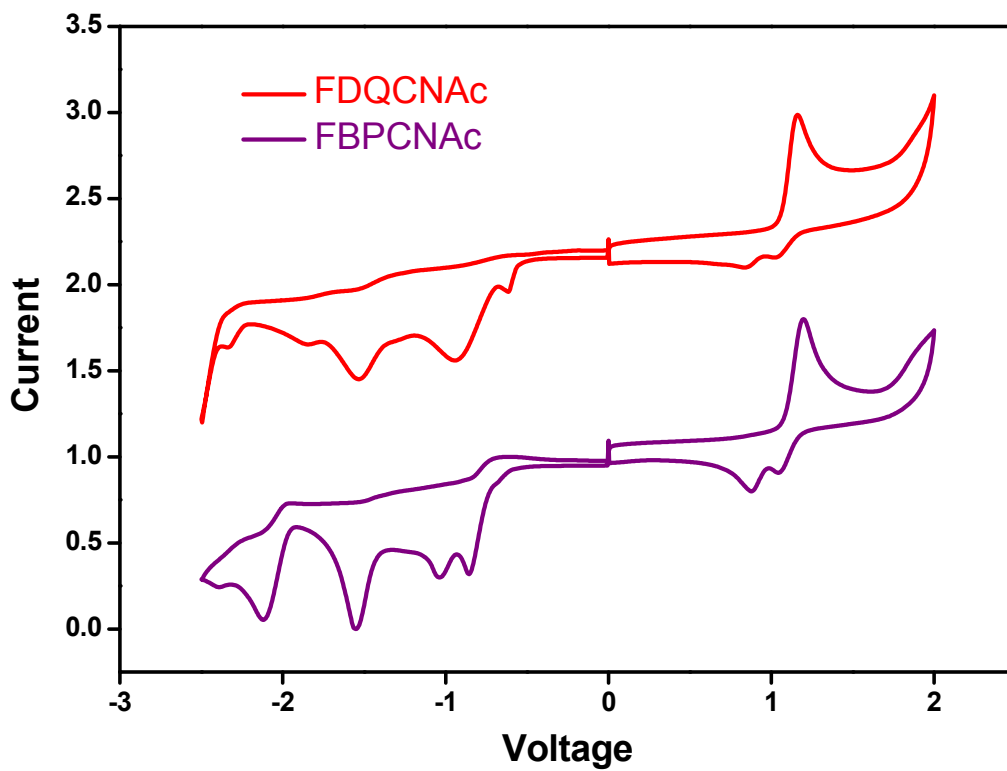


Figure S4. Cyclic voltammograms of TADF emitters FDQCNAC and FBPCNAC.

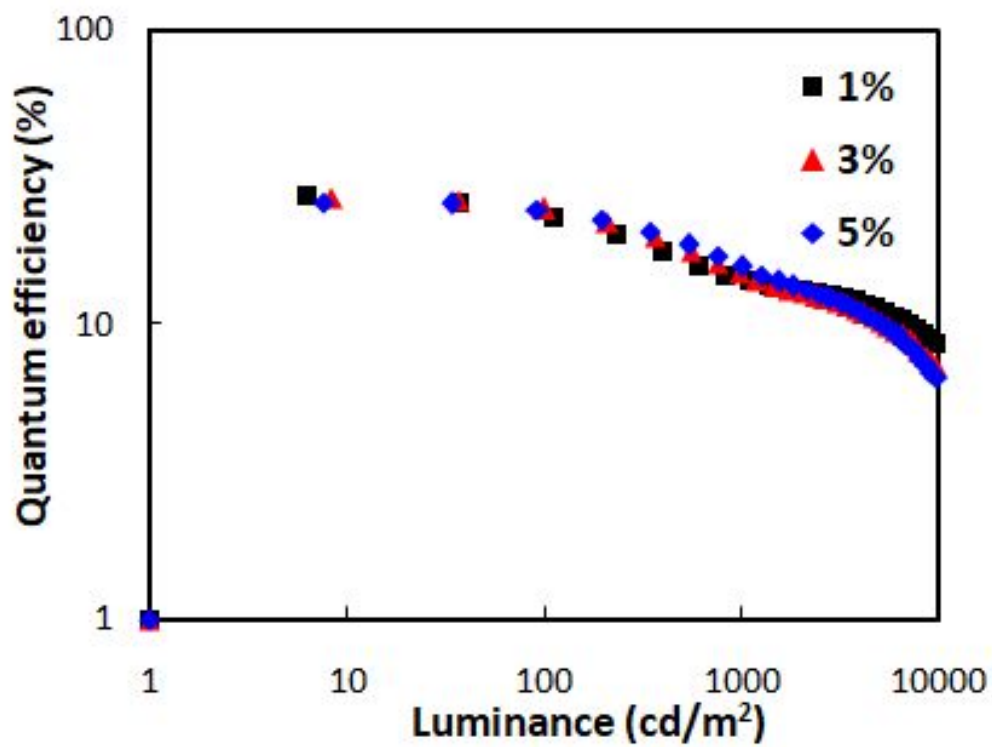


Figure S5. EQE–luminance curves of FDQCNAC doped OLED (1-5 %)

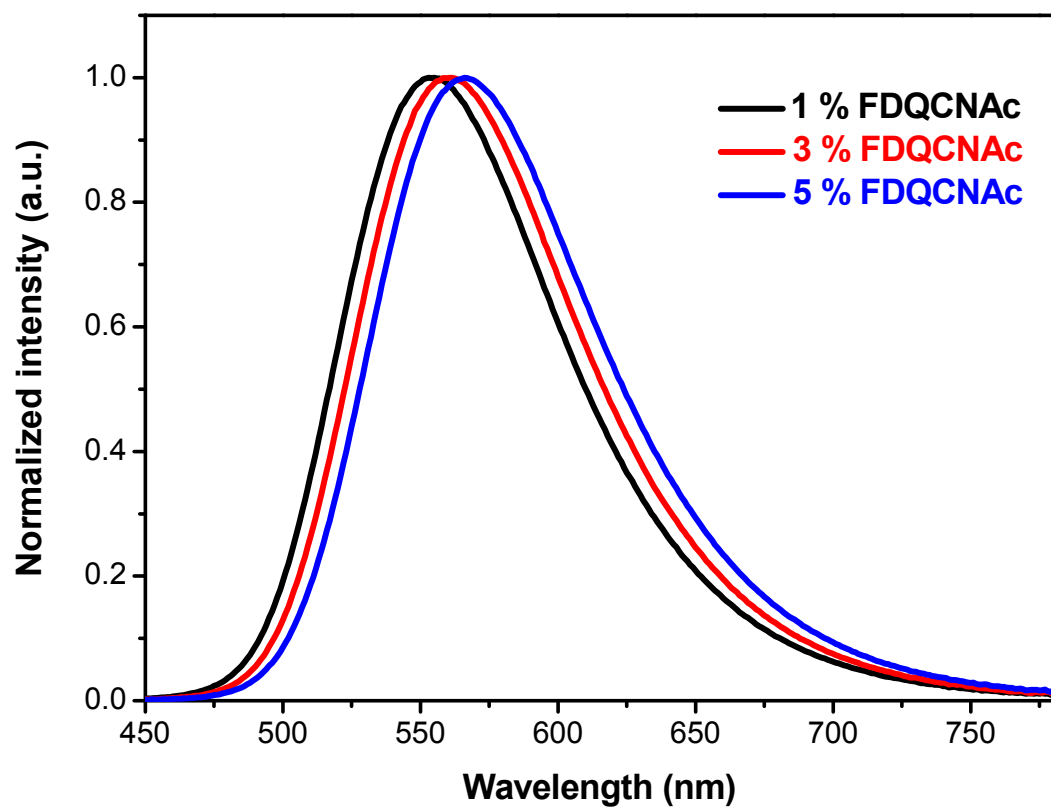


Figure S6. EL spectra of FDQCNAC at 1-5 % doping concentration

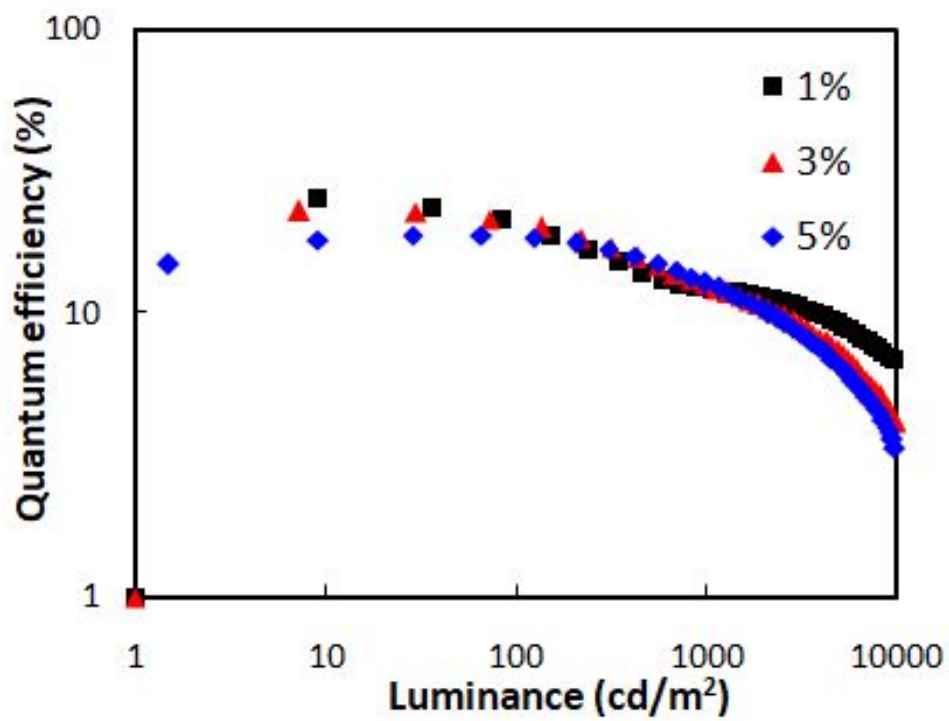


Figure S7. EQE–luminance curves of FBPCNAc doped OLED (1-5 %)

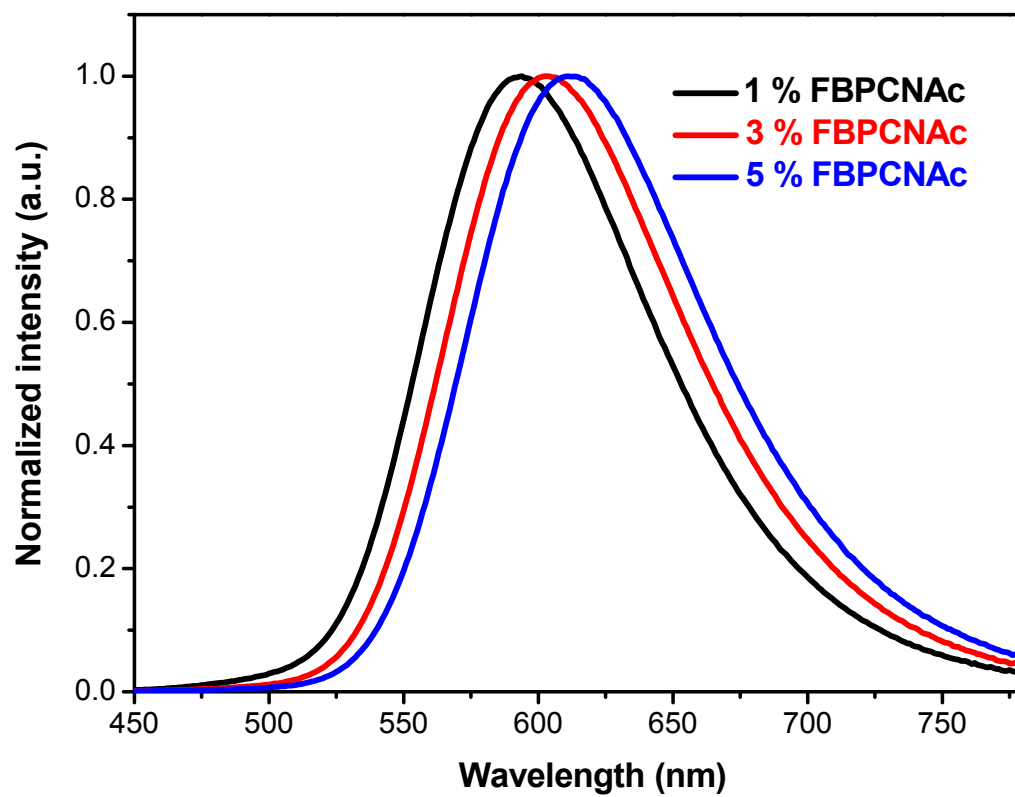


Figure S8. EL spectra of FBPCNAc at 1-5 % doping concentration

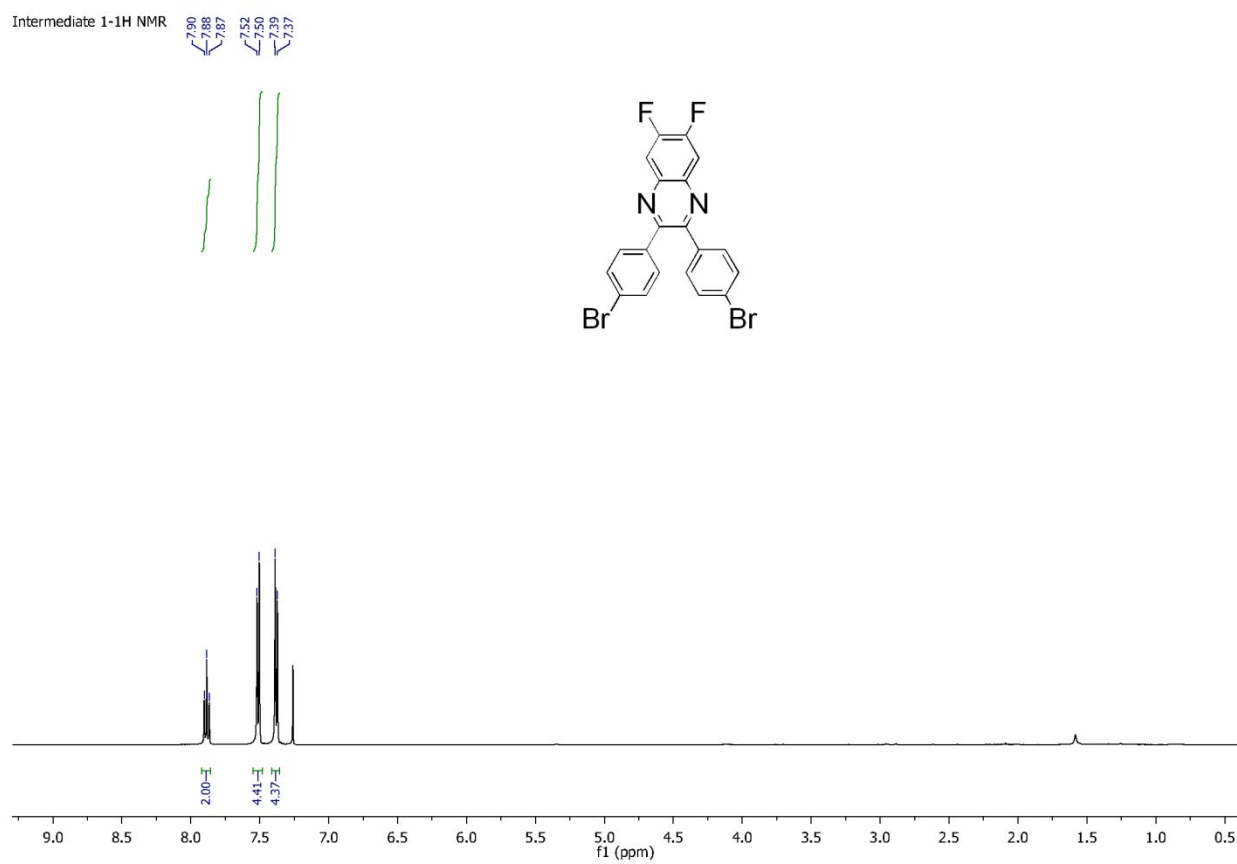


Figure S9. ¹H NMR spectrum of Intermediate 1

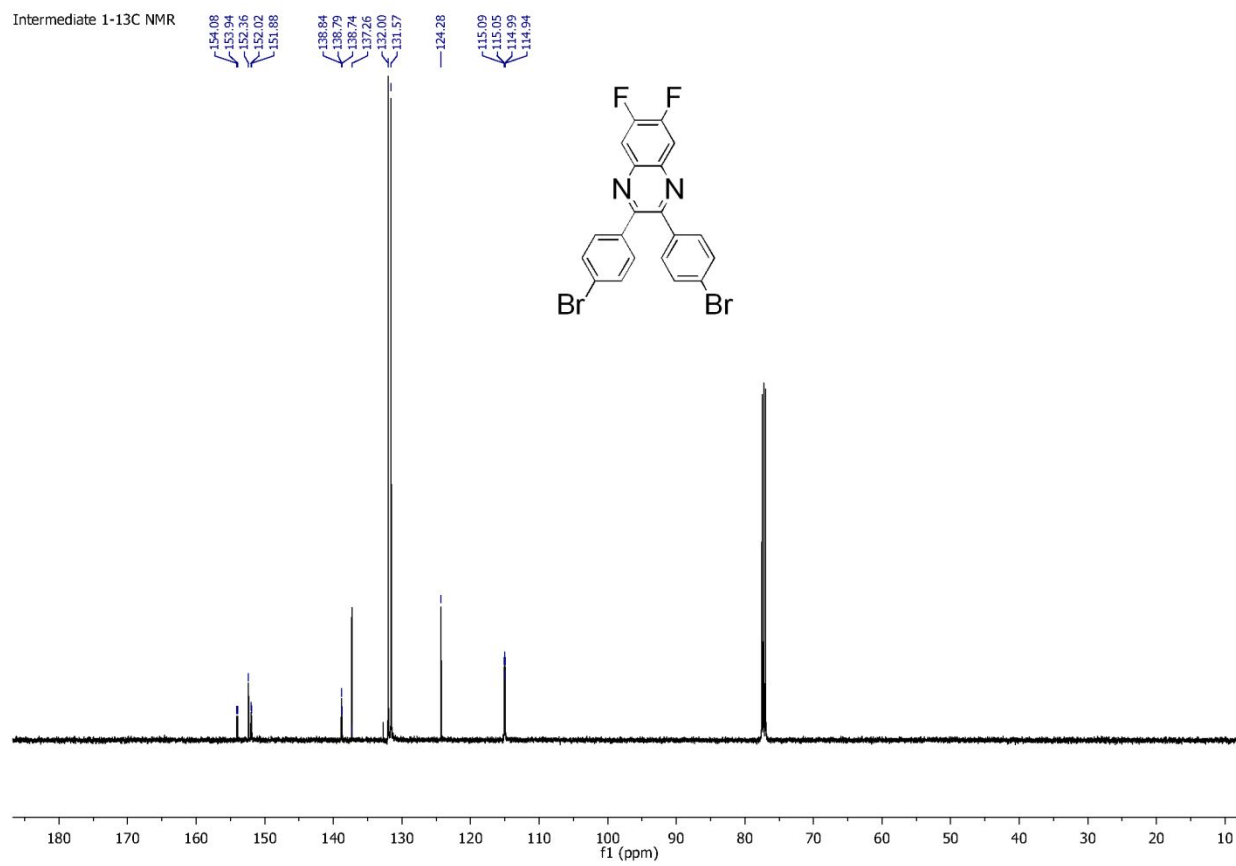


Figure S10. ¹³C NMR spectrum of Intermediate 1

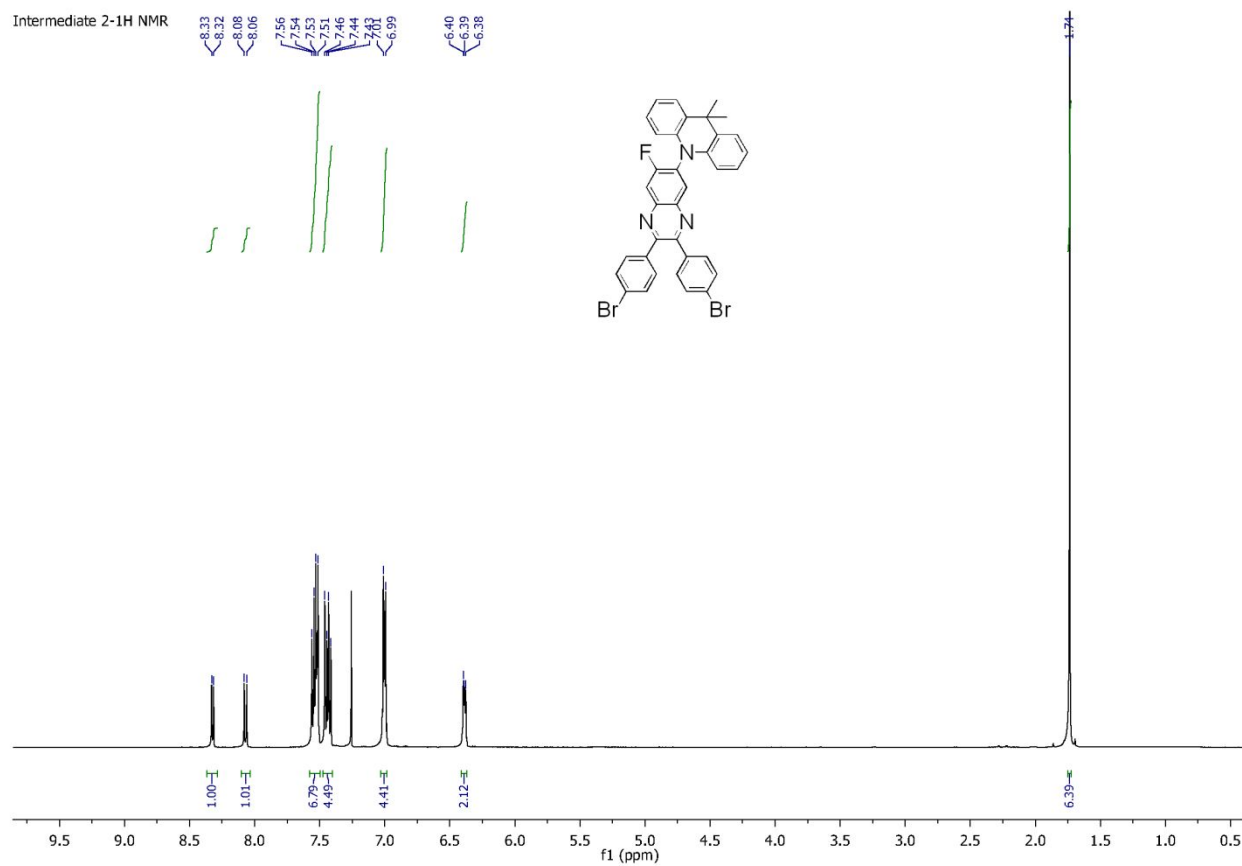


Figure S11. ¹H NMR spectrum of Intermediate 2

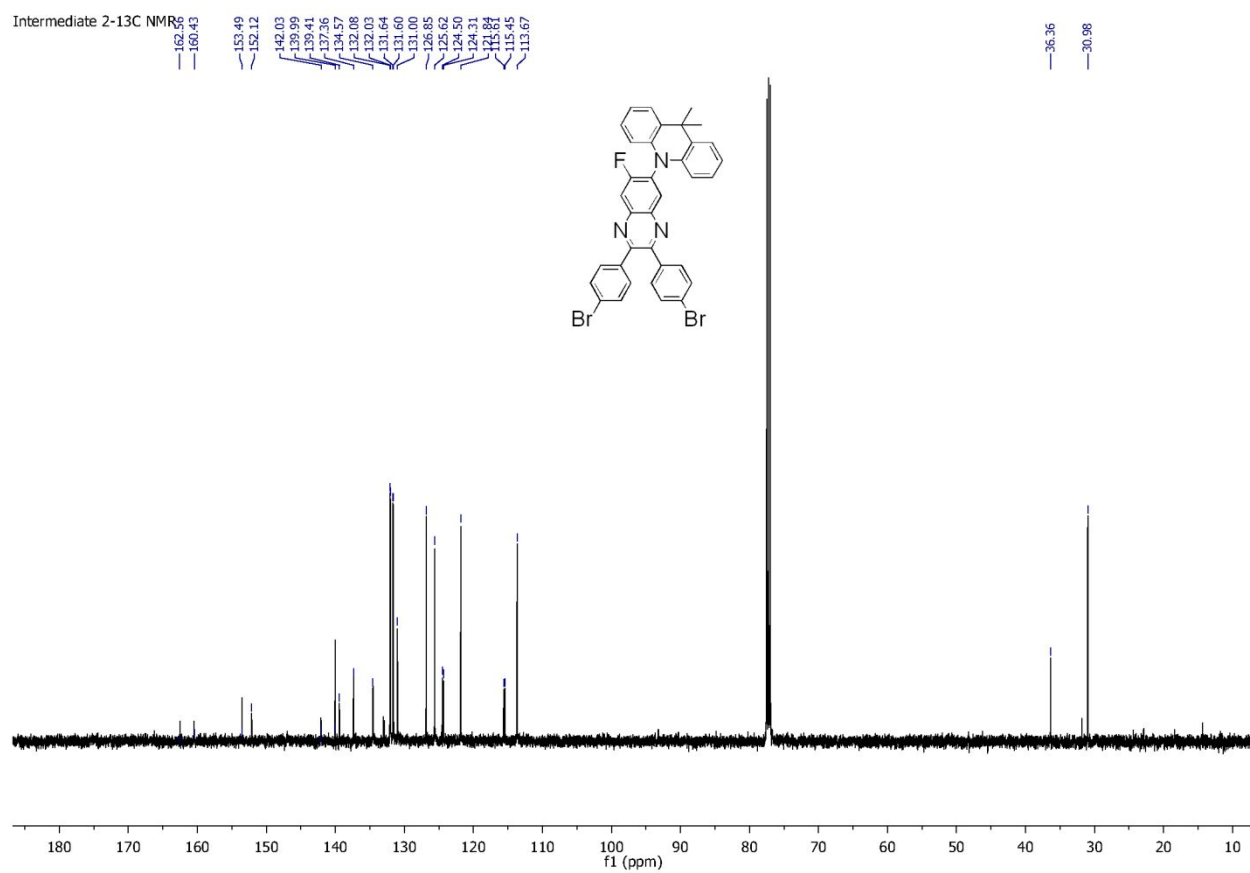


Figure S12. ¹³C NMR spectrum of Intermediate 2

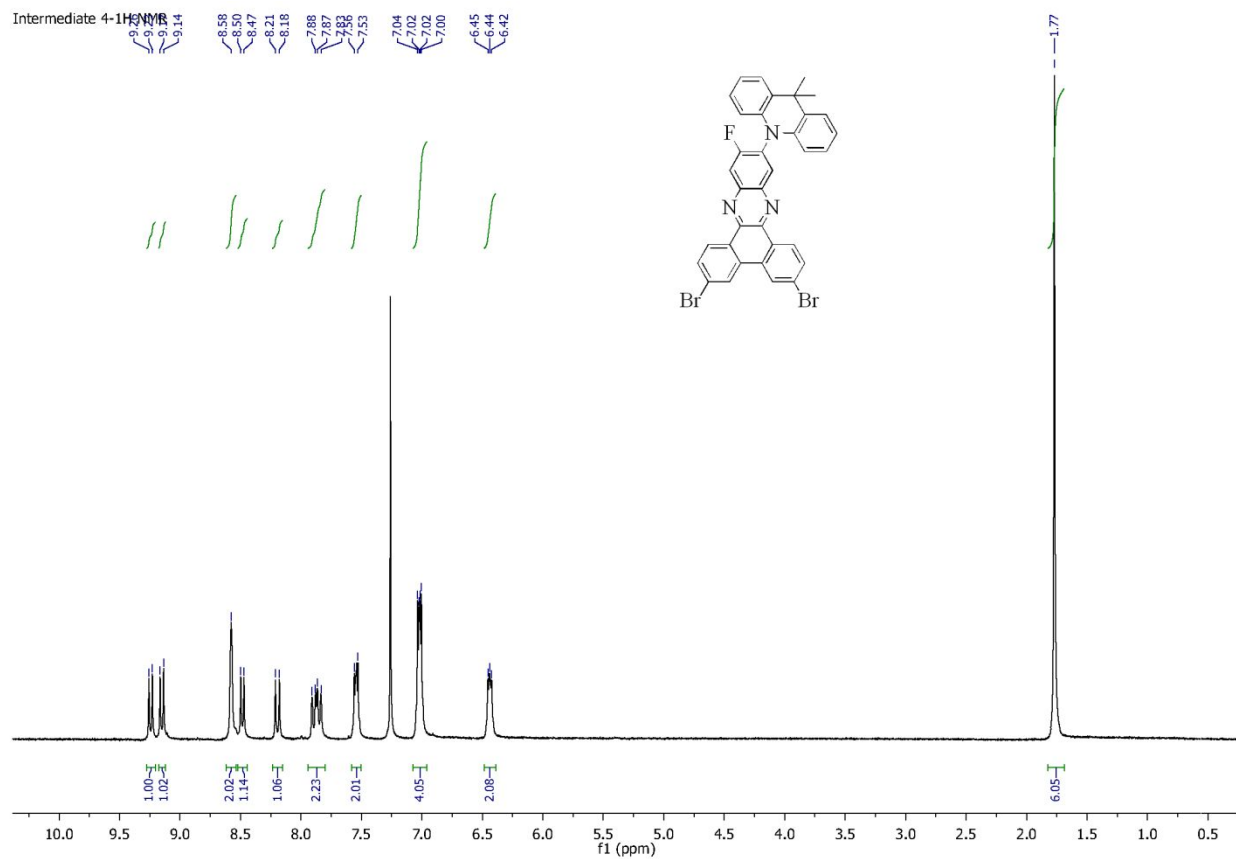


Figure S13. ¹H NMR spectrum of Intermediate 4

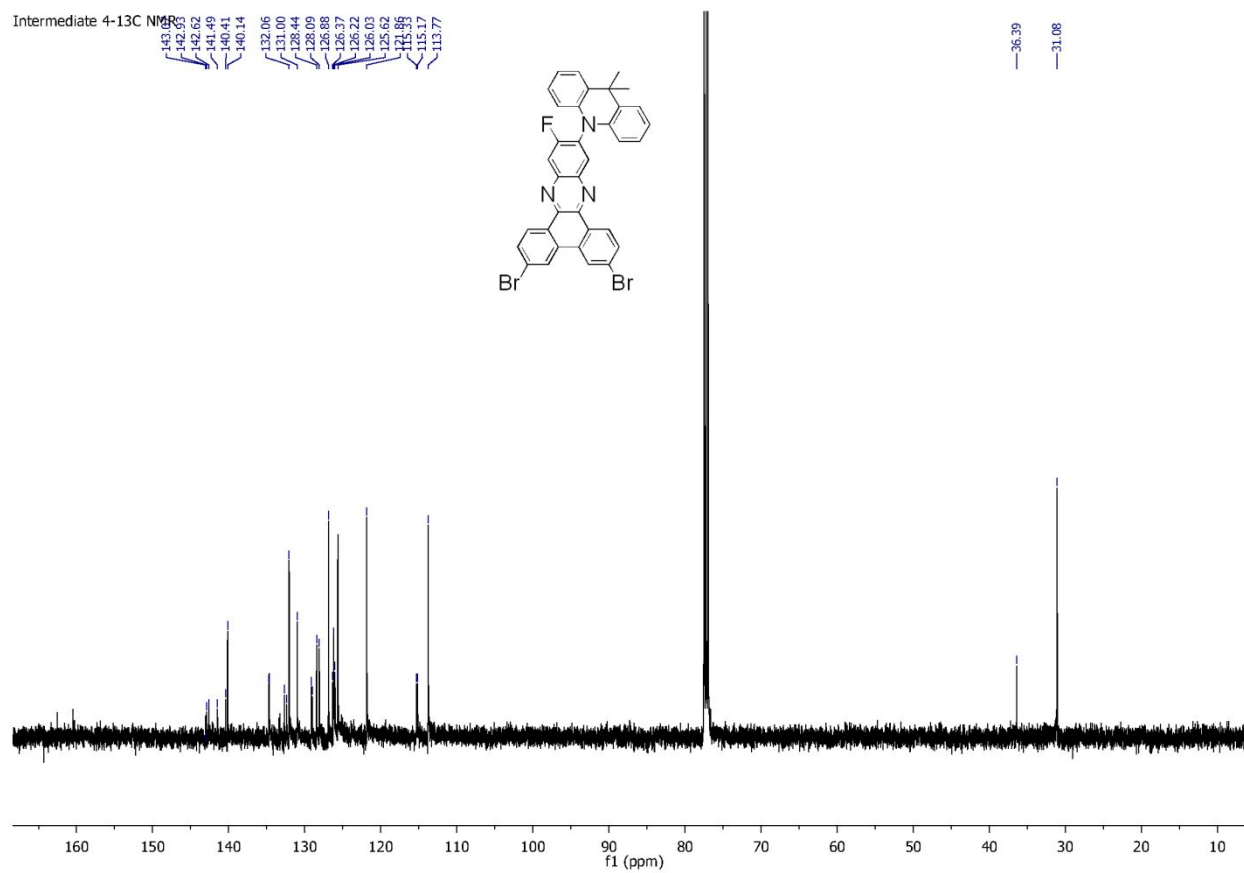


Figure S14. ¹³C NMR spectrum of Intermediate 4

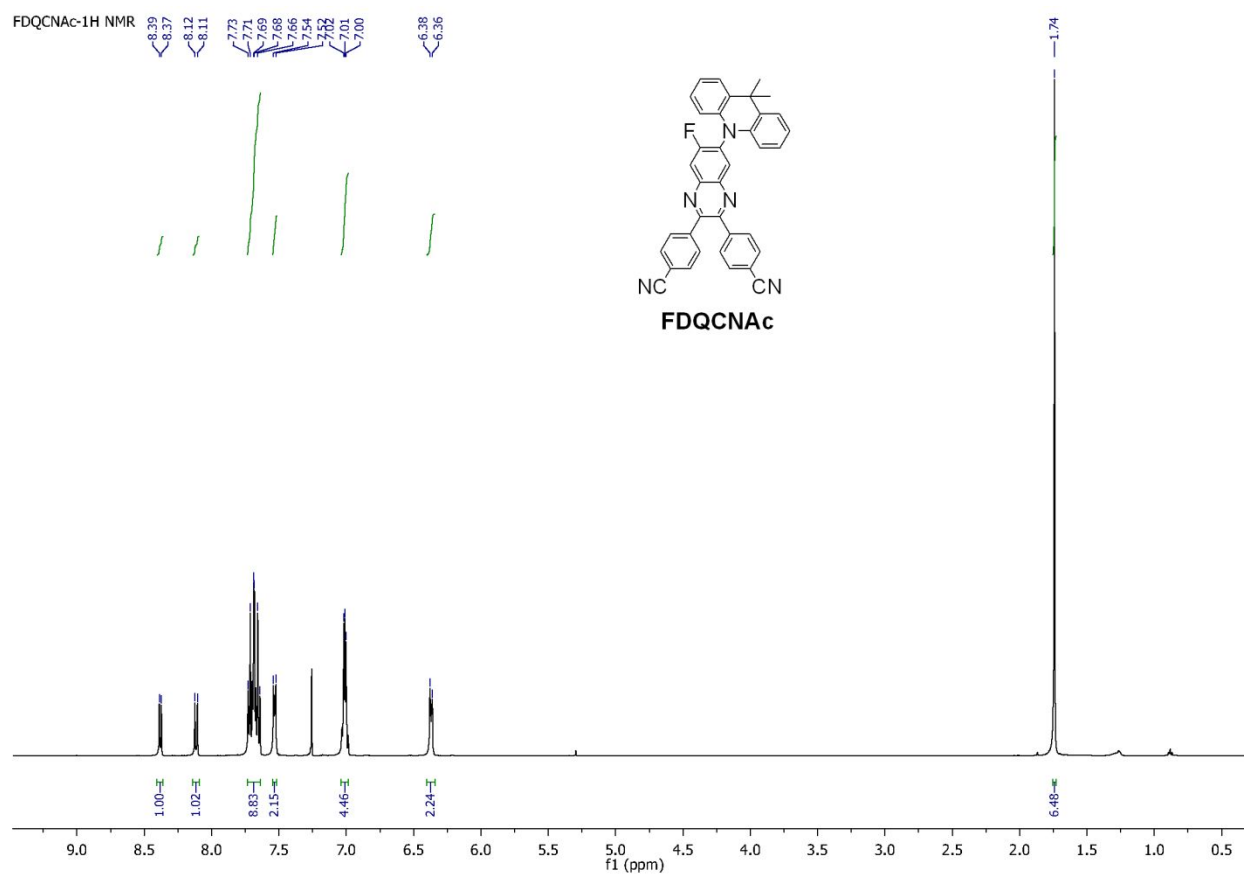


Figure S15. ¹H NMR spectrum of FDQCNAc

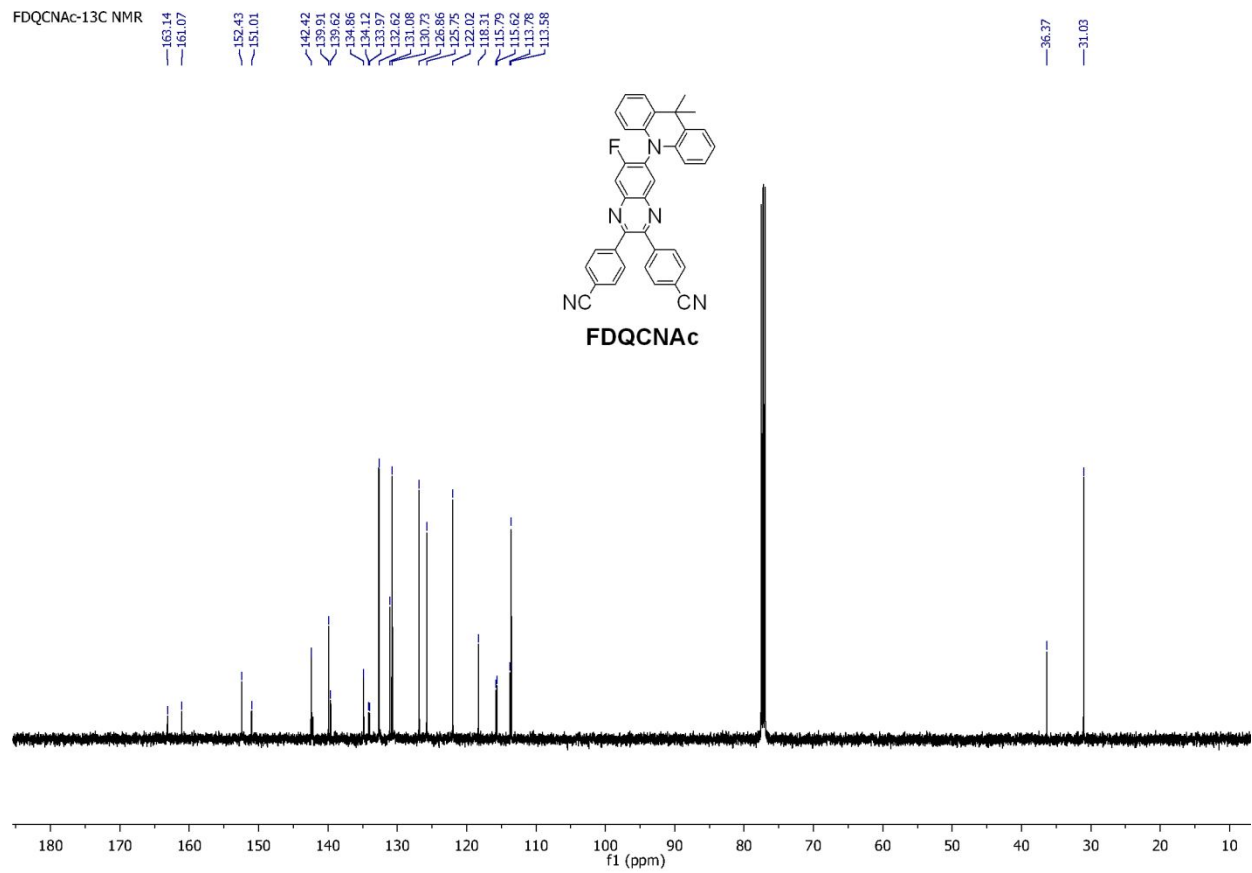


Figure S16. ¹³C NMR spectrum of FDQCNAc

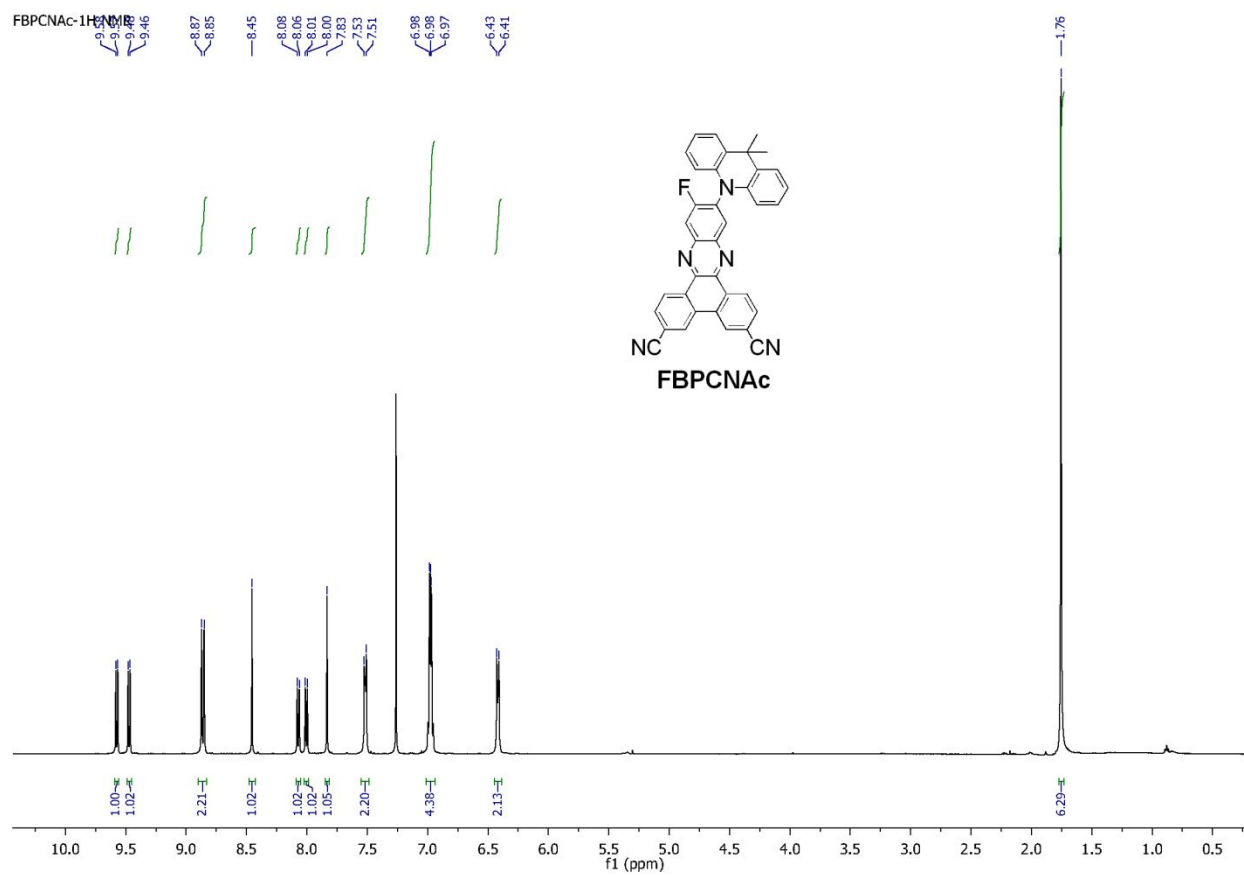


Figure S17. ^1H NMR spectrum of FBPCNAc

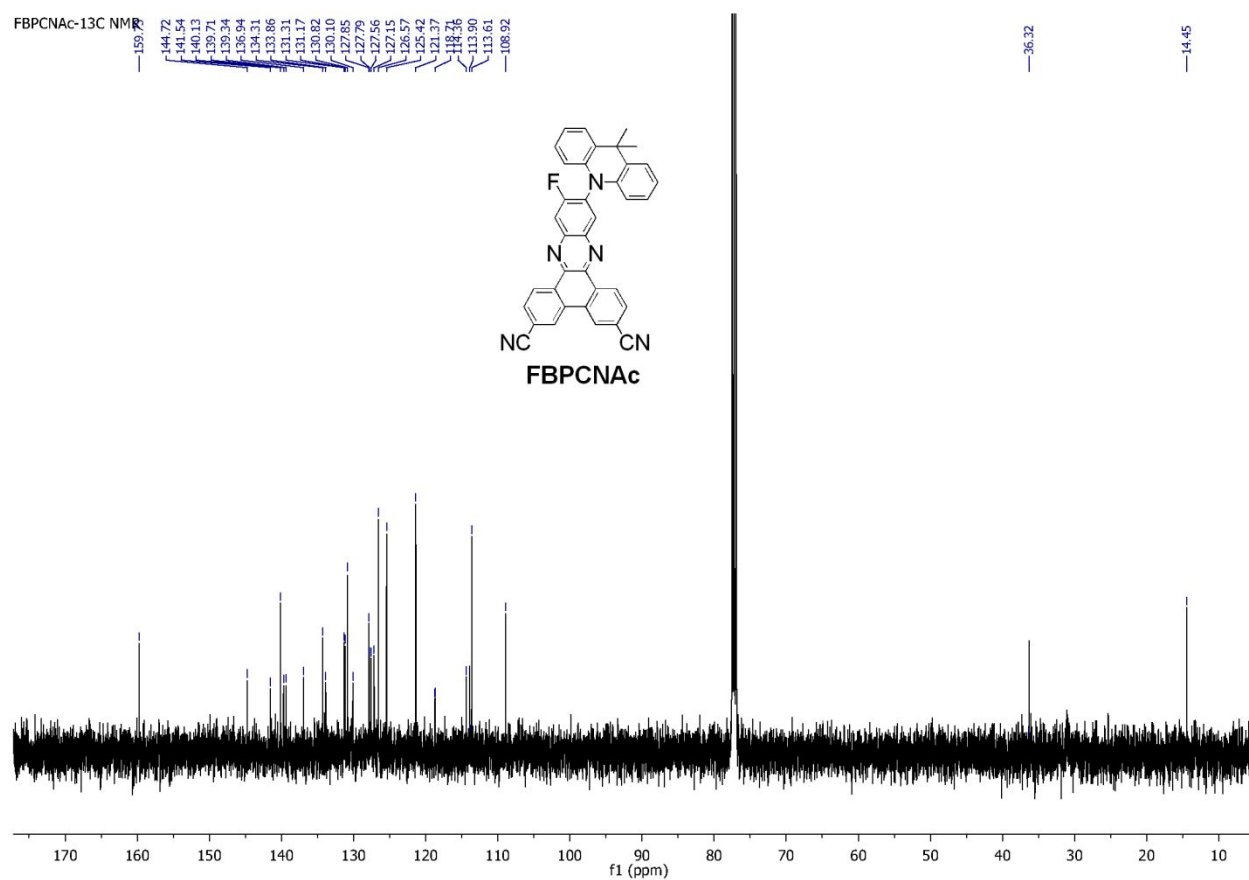


Figure S18. ^{13}C NMR spectrum of FBPCNAc

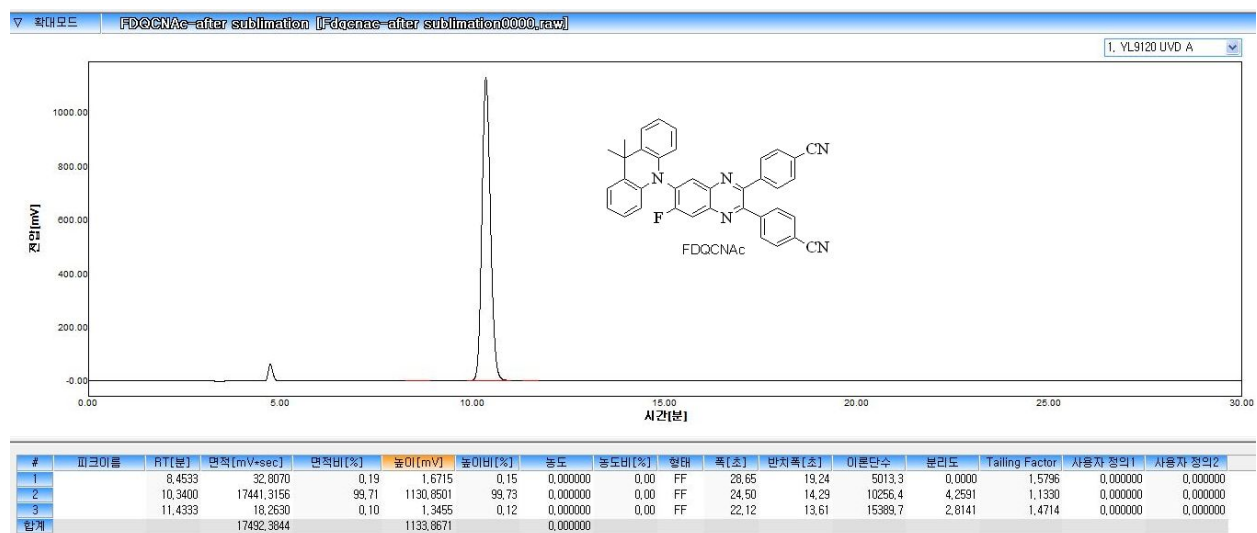


Figure S19. HPLC report of FDQCNAc after sublimation.

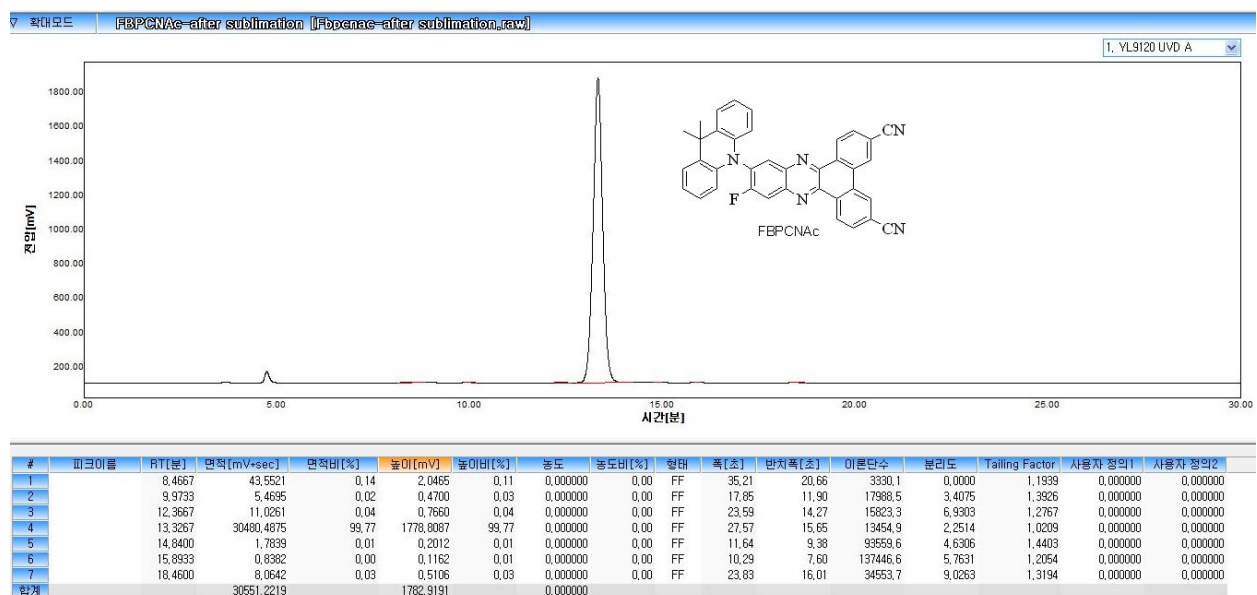


Figure S20. HPLC report of FBPCNAc after sublimation.

Data : FAB735 Date : 30-Jan-2020 21:25

Instrument : MStation

Sample : KSS-38

Note : m-NBA

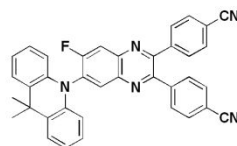
Inlet : Direct Ion Mode : FAB+

RT : 0.39 min Scan# : (14,20)

Elements : C 100/0, H 100/0, F 2/0, N 10/0

Mass Tolerance : 1000ppm, 5mmu if m/z < 5, 10mmu if m/z > 10

Unsaturation (U.S.) : 20.0 - 35.0



Chemical Formula: C₃₇H₂₄FN₅
Exact Mass: 557.2016

	Observed m/z	Int%	Err [ppm / mmu]	U.S.	Composition
1	558.2093	16.75	-11.8 / -6.6	27.0	C41 H28 F2
2			+10.7 / +6.0	27.5	C40 H26 F2 N
3			-0.5 / -0.3	31.0	C42 H26 N2
4			-0.2 / -0.1	27.5	C37 H25 F N5
5			+0.2 / +0.1	24.0	C32 H24 F2 N8
6			-11.0 / -6.2	27.5	C34 H24 N9
7			+11.5 / +6.4	28.0	C33 H22 N10

Figure S21. HRMS report of FDQCNAC.

Data : FAB836 Date : 26-Feb-2020 14:26

Instrument : MStation

Sample : KSS-24-1

Note : m-NBA

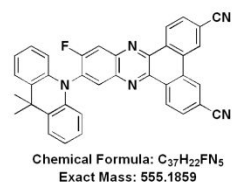
Inlet : Direct Ion Mode : FAB+

RT : 1.62 min Scan# : (55,239)

Elements : C 100/0, H 100/0, F 2/0, N 10/0

Mass Tolerance : 1000ppm, 5mmu if m/z < 5, 20mmu if m/z > 20

Unsaturation (U.S.) : 15.0 - 40.0



	Observed m/z	Int%	Err [ppm / mmu]	U.S.	Composition
1	556.1937	50.01	-11.8 / -6.6	28.0	C41 H26 F2
2			-23.1 / -12.8	31.5	C43 H26 N
3			+10.8 / +6.0	28.5	C40 H24 F2 N
4			-0.4 / -0.2	32.0	C42 H24 N2
5			+33.4 / +18.6	29.0	C39 H22 F2 N2
6			+22.2 / +12.3	32.5	C41 H22 N3
7			-22.7 / -12.6	28.0	C38 H25 F N4
8			-0.1 / -0.0	28.5	C37 H23 F N5
9			+22.5 / +12.5	29.0	C36 H21 F N6
10			-22.3 / -12.4	24.5	C33 H24 F2 N7
11			-33.6 / -18.7	28.0	C35 H24 N8
12			+0.3 / +0.2	25.0	C32 H22 F2 N8
13			-11.0 / -6.1	28.5	C34 H22 N9
14			+22.9 / +12.7	25.5	C31 H20 F2 N9
15			+11.6 / +6.5	29.0	C33 H20 N10

Figure S22. HRMS report of FBPCNAc.

Equations for the calculation of rate constants

$$\tau_p = 1/k_p \quad (1)$$

$$\tau_d = 1/k_d \quad (2)$$

$$k_{ISC} = (1-\Phi_F) \times k_p \quad (3)$$

$$k_{RISC} = (k_p k_d / k_{ISC}) \times (\Phi_{TADF} / \Phi_F) \quad (4)$$

$$k_r^S = k_p \Phi_F \quad (5)$$

$$k_{nr}^T = k_d - k_{RISC} \Phi_F \quad (6)$$

$$\Phi_F = \Phi_{O_2} \quad (7)$$

$$\Phi_{TADF} = \Phi_{N_2-O_2} \quad (8)$$